Ocean Systems Engineering, *Vol. 14, No. 2 (2024) 157-169*
https://doi.org/10.12989/ose.2024.14.2.157

Finding the optimum shape of the energy dissipator to minimize the impact force due to the dam break flow

Asrini Chrysanti[1a] and Sangyoung Son[*2]

[1]Graduate School of Water Resources Management, Faculty of Civil and Environmental Engineering, Institut Teknologi Bandung, Jalan Ganesha 10, Bandung 40132, West Java, Indonesia
[2]School of Civil, Environmental, and Architectural Engineering, Korea University, 45 Anam-ro, Seongbuk-gu, Seoul 02841, South Korea

(Received March 8, 2024, Revised May 20, 2024, Accepted May 30, 2024)

Abstract. The sudden release of water from a dam failure can trigger bores on a flat surface and exert substantial impact forces on structures. This flow poses a high-risk flood hazard to downstream urban areas, making it imperative to study its impact on structures and devise effective energy dissipators to mitigate its force. In this study, a combination of Genetic Algorithm optimization and numerical modeling is employed to identify the optimal energy dissipator. The analysis reveals that a round arc-shaped structure proves most effective, followed by a triangular shape. These shapes offer wide adaptability in terms of structure dimensions. Structures with higher elevation, especially those with round or triangular shapes, demonstrate superior energy dissipation capabilities. Conversely, square-shaped structures necessitate minimal height to minimize impact forces. The optimal width for dissipating energy is found to be 0.9 meters, allowing for effective wave run-up and propagation. Furthermore, the force exerted on structures increases with higher initial water levels, but diminishes with distance from the dam, highlighting the importance of placement in mitigating impact forces.

Keywords: dam break; energy dissipator; genetic algorithm; lateral force; optimization; structure shape

1. Introduction

A dam break flow, stemming from the abrupt collapse of a high dam and the subsequent uncontrolled release of impounded water, constitutes a catastrophic event. The instantaneous free surface flow profiles of such occurrences exhibit similarities to tsunami flows, capable of inducing bores on horizontal beds and exerting high impact forces (Chanson 2006, Jung and Son 2023, Son and Jung 2022). This type of flood poses a significant risk to urban areas situated along downstream riverines, particularly as urbanization encroaches upon dam locations, heightening the potential for catastrophic disasters.

Understanding the dynamics of dam break flow around structures is paramount for effective disaster risk reduction efforts. The analysis of dam break flow has evolved from rudimentary to advanced numerical models, with most models employing shallow water equations (SWE) and recent advancements incorporating 3D modeling techniques (Hwang and Son 2023, Qian *et al*.

*Corresponding author, Professor, E-mail: sson@korea.ac.kr

http://www.techno-press.org/?journal=ose&subpage=7 ISSN: 2093-6702 (Print), 2093-677X (Online)

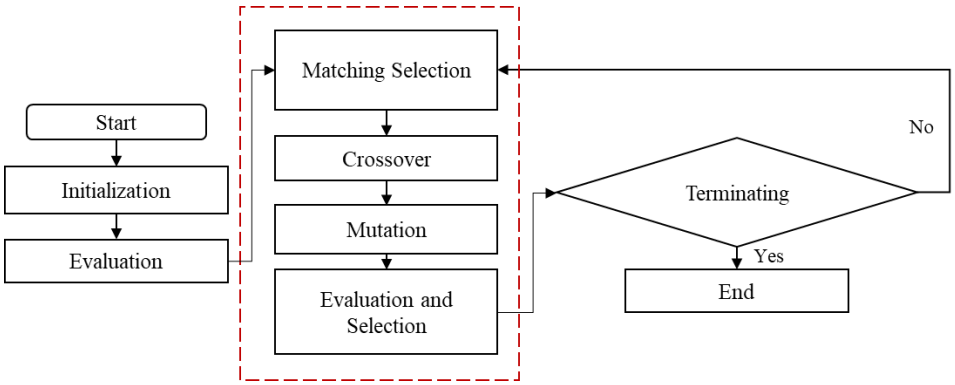

Fig. 1 Search methodology of a GA optimization model

2024). Despite varying degrees of complexity, numerical models, even those utilizing simplified equations, demonstrate good agreement with analytical and empirical data, underscoring their capability to replicate dam break flows (Soares-Frazão and Zech 2008, Putri *et al*. 2020, Noh and Son 2023, Chrysanti *et al*. 2023).

The study of dam break-structure interaction faces limitations due to the multitude of variables and parameters influencing dam break flow characteristics. Additionally, dam break models are inherently complex, incorporating nonlinear correlations among parameters. In response, optimization algorithms offer a means to identify optimal parameters and facilitate model tuning. This study integrates an optimization procedure with a numerical model to determine the optimal shape and layout of structures, serving as effective energy dissipators to mitigate the impact force of dam break flows.

2. Methodology

2.1 Genetic algorithm

The Genetic Algorithm (GA) is a meta-heuristic technique that employs stochastic search principles inspired by genetic populations. Initially proposed by Holland in 1975, GA has found wide adoption across various engineering applications, offering an effective and robust optimization approach. Central to GA are its genetic operators, comprising three main components: reproduction, crossover, and mutation. Reproduction involves selecting parents from a mating pool based on their fitness. Crossover entails exchanging segments of genetic information between two parent strings. Mutation introduces random changes, typically through bit-flipping, with a predetermined probability. The GA procedure is depicted in Fig. 1.

2.2 Numerical model

In this study, the one-dimensional Saint Venant Equation is employed, assuming a hydrostatic pressure distribution. By utilizing the governing equation in one dimension, computational time is minimized. The application of mass conservation and Newton's Second Law to the control volume

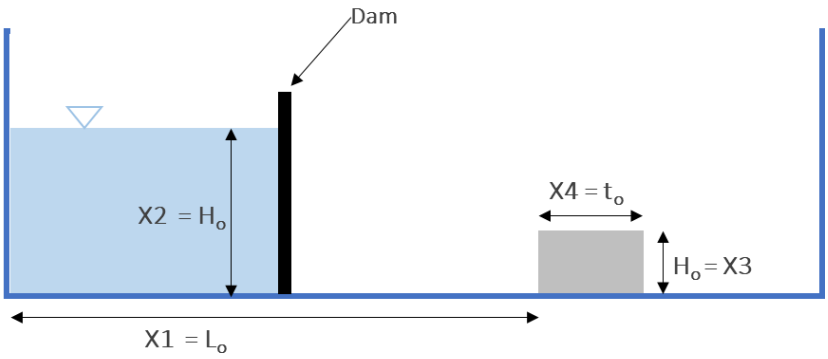

Fig. 2 Schematic illustration of idealized dam break model

yields the one-dimensional Saint Venant equations, comprising continuity (Eq. (1)) and momentum (Eq. (2)) equations, as follows

$$\frac{\partial h}{\partial t} + \frac{\partial (hu)}{\partial x} = 0 \tag{1}$$

$$\frac{\partial u}{\partial t} + u\frac{\partial u}{\partial x} = -g\frac{\partial h}{\partial x} + g\left(\frac{\partial (h+z)}{\partial x} - \frac{n^2 u|u|}{h^{\frac{4}{3}}}\right) \tag{2}$$

where u is the velocity, h is water depth, g is gravitational acceleration, z is the bed level. The proposed numerical scheme uses the finite difference method (FDM) for discretizing the Saint Venant Equation. The second-order accurate of Lax-Wendroff scheme is applied in both time and space. To avoid the Jacobian matrix in the solving evaluation, two-step procedure is developed. The first procedure of Lax's follows at the half timestep and half grid and continues the second procedure of Wendroff's step at the next timestep. Both procedures are described in Eqs. (3)-(5). The Lax's Step

$$u_{i+1/2}^{n+1/2} = \frac{1}{2}(u_{i+1}^{n} - u_{i}^{n}) - \frac{\Delta t}{2\,\Delta x}(f(u_{i+1}^{n}) - f(u_{i}^{n})) \tag{3}$$

$$u_{i-\frac{1}{2}}^{n+\frac{1}{2}} = \frac{1}{2}(u_{i}^{n} - u_{i-1}^{n}) - \frac{\Delta t}{2\,\Delta x}(f(u_{i}^{n}) - f(u_{i-1}^{n})) \tag{4}$$

Wendroff Step

$$u_{i}^{n+1} = u_{i}^{n} - \frac{\Delta t}{\Delta x}\left(f(u_{i+\frac{1}{2}}^{n+\frac{1}{2}}) - f(u_{i-\frac{1}{2}}^{n+\frac{1}{2}})\right) \tag{5}$$

where f denotes the discretized function based on the momentum equation. Since the Lax-Wendroff scheme is noted as an unconditionally stable condition, the stability of the numerical model is governed by the CFL (Courant-Friedrich-Lewy) criterion which satisfied $|CFL|\ \Delta t/\Delta x < 1$. To further reduce the numerical instability, the numerical filter was adapted to reduce the oscillation by the high gradient and discontinuity of a shock wave. The Hansen filter was adopted as a dissipator and applied at each timestep of all grid domains. Hansen filter described in Eq. (6) with the parameter C is set to 0.98. The filter is applied to both parameters' velocity and water depth.

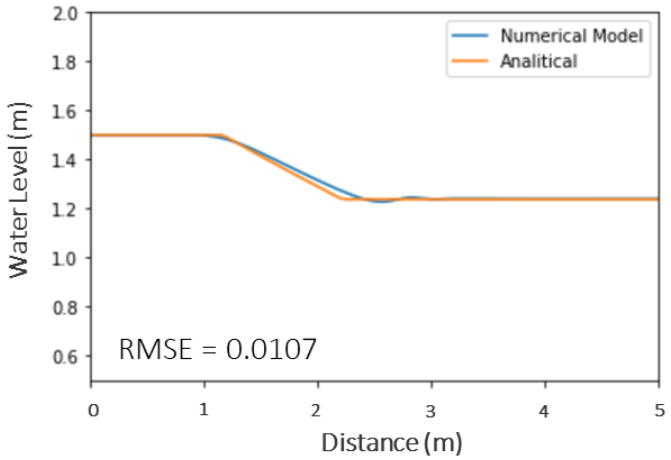

Fig. 3 Model validation with analytical result

$$f_i = Cf_i + 0.25(1 - C)(f_{i-1} + f_i + f_{i+1}) \tag{6}$$

The schematic diagram of the idealized dam break model is illustrated in Fig. 2. Prior to the application of the optimization, the numerical model is validated using the analytical solution described in Delestre *et al.* (2013) for a dam break case on a wet domain without friction. The result can be seen in Fig.3. The result shows good agreement with a relatively low root mean square error (RMSE) of 0.0107.

2.3 Coupled GA-numerical model

To evaluate the optimum energy dissipator of a dam break flow, the force acting on the structure was evaluated as the fitness function. The force (hydrostatic load and momentum flux term) per unit width calculated at the nodes adjacent to the structure (0.05 m from the structure surface) estimated by the equation

$$Minimize \quad f(h,u) = \rho g \frac{h^2}{2} + \rho h|u|^2 \tag{7}$$

The force exerted in the structure is calculated based on the assumption of hydrostatic pressure and the net force perpendicular to the wall of the structure. The force exerted in the structure is calculated for every time step for every iteration. The water depth and velocity for the obtained minimum force is then abstracted. The decision variables and constraints are consisting of five variables described in Table 1.

The numerical domain was set using the length of 2.5 m, with the grid spacing (Δx) of 0.05 m and the time interval (Δt) of 0.01 second. The initial dam water level was initiated at the left side of the domain with the fixed water column width set to 0.4 m. The structure of the energy dissipator was set as the bed level in the computational domain. Each randomly generated shape will create a bed level with random decision variables of structure dimension and location. The computational domain and each energy dissipator shape are described in Fig. 4. The x-axis

Table 1 Decision variables and variable constraint

Decision variables	Constraint
X_1 = Obstacle location from the dam: L_o (m)	1 – 2
X_2 = Initial dam water level: H_i (m)	0.2 – 2
X_3 = Structure dimensions (height): h_o (m)	0.2 -1
X_4 = Structure dimensions (width): t_o (m)	0.2 -1
X_5 = Obstacle Shape	'Square', 'Triangle', 'Round'
Degree for the triangle shape	20^0 – 60^0
Non-negativity constraints, all the variables (X_1, X_2, X_3, X_4, $X_{5\,(angle)}$) > 0	

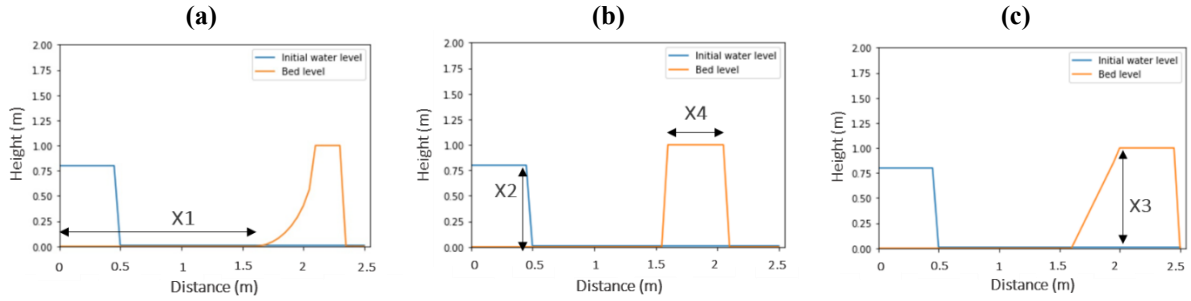

Fig. 1 Grid domain set-up with random choice of energy dissipator shape for round (a), square (b) and triangle (c) shape

described the distance, and the y-axis denoted the height of water level and bed level. Each decision variable also illustrated in the figure.

The numerical model and GA then coupled, exchanging information of the new population of decision variables and the result of the numerical dam break model. The information exchanged is performed in the post-processing step of calculating the water depth and velocity within the structure surface based on the initiation of model initial condition by GA. The input matrix (initial condition) then replaced by the combination of variables resulted from numerical model and deciding parameters to proceed for population evaluation in the GA. The fitness is then calculated based on the numerical model result. GA algorithm continues with the evaluation and selection using the fitness value and continues to the genetic operator. The GA algorithm will terminate after the iteration step is fulfilled. The coupled GA-Numerical model framework can be seen in Fig. 5.

3. Result and discussion

Three optimization procedures will be investigated in this study. Since five variables are determined as the deciding parameters, solving all parameters at once may be difficult to obtain the globally optimal result and not achieve convergence. Three optimization procedures are shown in Fig. 6 and described as follows:

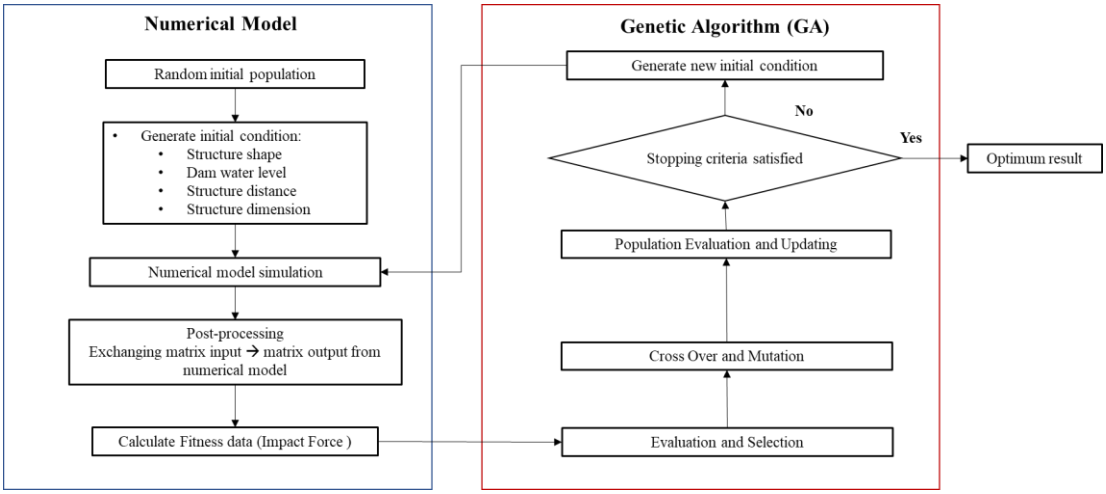

Fig. 5 The GA-Numerical model coupled framework

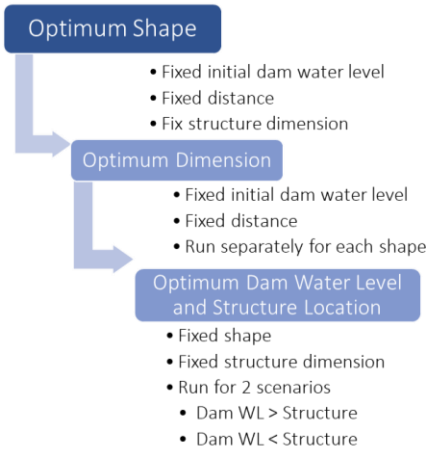

Fig. 6 Optimization procedure

Table 2 Input parameter value used in GA

Scenario	Structure Shape	Structure Dimension	Dam initial WL and distance
Maximum number of iterations in GA	100	1000	100
Generation runs	1	3	10
Population size	4	4	4
Mutation probability in GA (P_m)	0.1	0.1	0.1
Crossover probability in GA (P_c)	0.8	0.8	0.8

• *Optimum structure shape*: The shape of the structure is the decision variables, which will be generated randomly at each generation. Once the triangle shape of the structure is selected. The random angle will be generated randomly ranging from 200 to 600. The water level and structure distance are fixed at 1.5 m and 1 m respectively. The dimensions also remain fixed with the dimension of 0.5 m (height) x 0.5 m (width/radius).

• *Optimum structure dimension*: The optimum dimension of the energy dissipator will be investigated for each shape. The reason for separated investigation in this procedure is since each shape has a different characteristic to the wave generated and wave propagation. The initial water level and structure distance from the dam are set to fixed remain similar to the first procedure.

• *Optimum initial dam water level and structure location*: The last procedure is investigating the effect of dam water level and the structure distance from the dam. The shape of the structure is selected using the optimum shape resulted from the first procedure. The dimension remains fixed at 0.5 m (height) x 0.5 m (radius).

Since each procedure has a different number of decision variables and the uncertainty of water flows characteristics, the number of iterations and generation runs adapted on each procedure. However, the minimum number of iterations of all runs is set to be 1000 for each optimization procedure. The number of iterations, generation runs, and another parameter used in GA is given in Table 2.

3.1 Optimum structure shape

The initial optimization process aims to explore the impact of structure shape as an energy dissipator. This optimization runs for a single generation comprising 1000 iterations. Given that only one variable serves as the decision variable, one generation is deemed sufficient. Despite considering the angle of the triangular shape in this optimization, the results quickly converge to an optimal solution within five iterations, evident in Fig. 7.

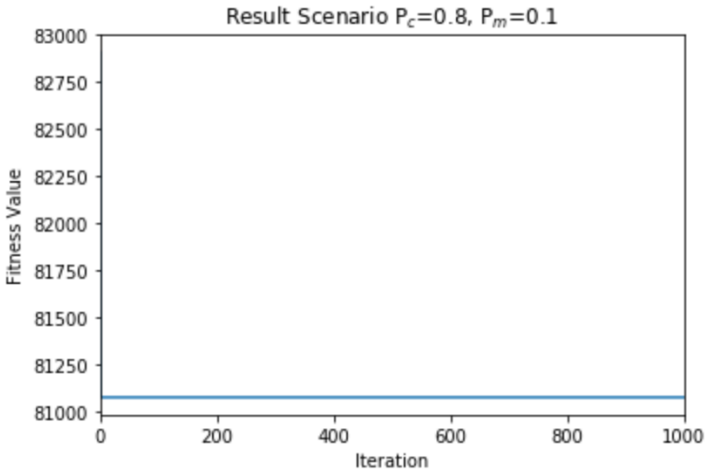

Fig. 7 Fitness variation in optimizing structure shape

Table 1 Minimum force of each structure shape

Structure Shape	Minimum Force (N)
Square	87449.13
Round	80997.25
Triangle	82723.81

To obtain a more precise understanding of the impact of structure shape on exerted force, the minimum force for each shape resulting from these iterations is tabulated in Table 3. It's evident that the square shape yields the highest force due to the intense vertical impact on the structure, resulting in high momentum. Conversely, the triangular shape proves to be a competent energy dissipator, resulting in relatively lower force compared to the square shape. Remarkably, the round shape exhibits the minimum force at 80 kN. These findings align with previous research in similar domains.

Issakov *et al*. (2019) investigated optimal structures to minimize maximum pressure through numerical simulations utilizing the Volume of Fluid (VOF) method. Their study noted that arch-shaped structures may reduce pressure by 2.5 – 3 times compared to triangular shapes. The study shows that maximum pressure exerted on the square structure at the first collision, while the arched structure provides more pressure distribution on structure surface. The arc shape of the structure facilitates easy water propagation, effectively reducing force-velocity during this process. Notably, velocity plays a significant role in force generation, as discerned from Eq. (7). Similarly, Saghi *et al.* (2019) explored various shapes using the VOF model and analyzed forces via entropy generation analysis. Their results identified a triangular shape with a 55° angle as the optimal dissipator. However, it's worth noting that while their study considered a semi-circular upward-rounded shape, the round structure in our study features an arc acting downward, akin to the study by Issakov *et al.* (2019).

3.2 Optimum structure dimension

The optimization of structure dimension may be the most difficult part to find the optimum solution. Since the triangle and round are also identified to have a significant reduction effect, generation runs of all shapes together may not be able to find the global optimum solution. The optimization generation is conducted on each separate shape. Each shape is run for the total number of iterations is 3000, which consists of 1000 iteration of 3 generation runs (Fig. 8). The fitness value of each shape could be achieved by multiple combinations of structure dimensions We collected 30 data of best fitness from all shape and plot the structure dimension in Fig. 9.

Remarkably, from the simulation runs, it's notable that all shapes yield the same width, measuring 0.9 m (Fig. 9). This finding suggests that the structure deck may function as a facilitator for wave runup. However, the height of the structures varies among different shapes. To delve deeper into the impact of building dimensions, this study employs the building ratio, defined as the structure height divided by its width. Despite the force exerted on the structures converging to similar values, the building dimensions, particularly for round and triangular shapes, exhibit variability.

The square structure demonstrates the most consistent pattern, with the lowest structure height resulting in minimum force. In contrast, the triangular shape exhibits varied structure heights

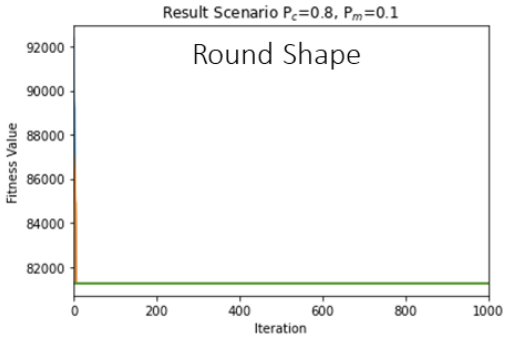

(a) Round shape

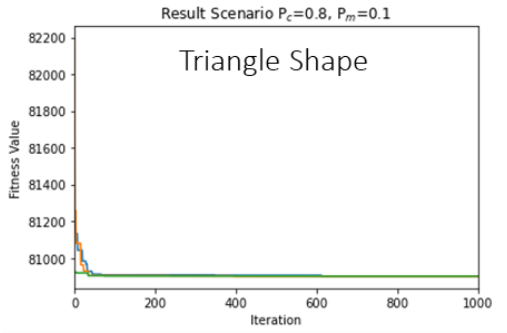

(b) Triangle shape

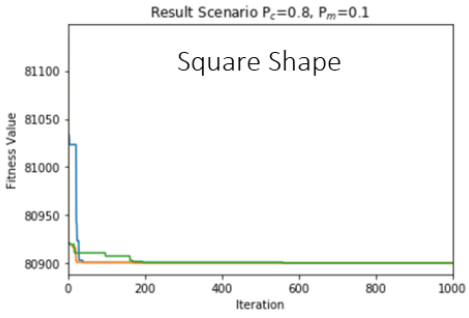

(a) Square shape

Fig 8 Fitness variation in optimizing structure dimension of (a) round shape; (b) triangle shape and (c) square shape.

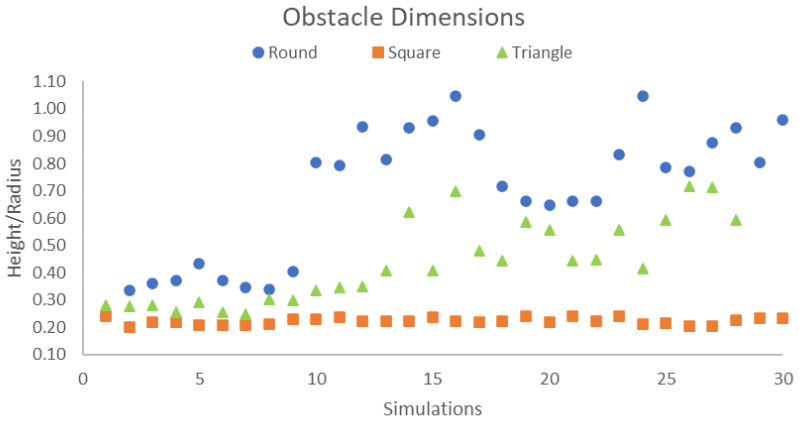

Fig. 9 Variation of structure dimension on the minimum force acting on the structure

ranging from 0.2 m to 0.6 m. The round shape displays a wider range of structure heights, spanning from 0.2 m to 0.9 m. This observed pattern elucidates the energy dissipation potential inherent in each shape,

consistent as discussed in the preceding section. The square shape, being the least efficient dissipator, necessitates minimizing structure height to mitigate impact forces. Conversely, the triangular shape, as highlighted earlier, demonstrates effective force reduction, allowing for higher structure dimensions while still significantly reducing impact forces. The round shape, recognized as the most proficient energy dissipator, accommodates a broader range of structural dimensions. Consequently, even at maximum dimensions (height equal to width), significant energy dissipation occurs.

3.3 Optimum dam initial water level and structure location

The final optimization procedure aims to explore the influence of both the initial dam water level and the location of the structure on impact force. This procedure is divided into two sections. In the first section, optimization is conducted with the initial dam water level set below the height of the structure (0.5 m). Conversely, the second section investigates scenarios where the initial dam water level exceeds the height of the structure. Each section runs for 100 iterations across 10 generations, resulting in a total of 1000 iterations per section. The fitness variation for each section's individual runs is illustrated in Figs. 10(a) and 10(b).

The impact of the initial dam water level in both scenarios exhibits a consistent trend: as the initial water level increases, so does the force exerted. The force exerted where the obstacle height is higher than the dam water level, the force exerted almost half (25,857 N) than the lower obstacle (49,190 N) (refer to Figs. 10(c) and 10(e) axis value). Thus, when the initial dam water level is lower than the structure, the force reduction is approximately 53%. This trend aligns with findings from prior studies (Phin 2018). Consequently, to minimize force exertion, the structure's height must exceed the initial dam water level. However, this trend's significant impact is only apparent when the initial dam water level surpasses the structure's height. Negative slope observed for the cases where dam water level surpasses the structure's height, indicating an opposite trend.

The analysis of structure distance across both generations reveals a consistent trend: increased distance from the structure correlates with increased force exertion. While this outcome might seem intuitive, it is essential to note that the furthest distance from the obstacle does not invariably guarantee minimal force. Liu *et al*. (2018) shows the opposing result where the force exerted could be significantly reduced when the structure is placed downstream. However, Liu *et al.* (2018) also suggests that the distance have more significant influence in changing the proportion of velocity-induced force or pressure force acting on the structure. The efficacy of distance in mitigating force relies heavily on flow characteristics, particularly influenced by the dam water level. Achieving minimum force on a distant structure hinges on specific flow phenomena, such as hydraulic jump and maximum velocity occurrence, preceding the arrival of the dam break flow at the structure. In essence, optimal force reduction is attained when these critical flow dynamics manifest before reaching the structure. It also should be noted that our optimization is performed simultaneously for initial dam water level and structure distance.

4. Limitation and possible development

The investigation of dam break flows and their impact on structures remains a compelling area of research for many scholars. While this study has yielded several conclusions, it is crucial to acknowledge certain limitations and outline potential avenues for future development.

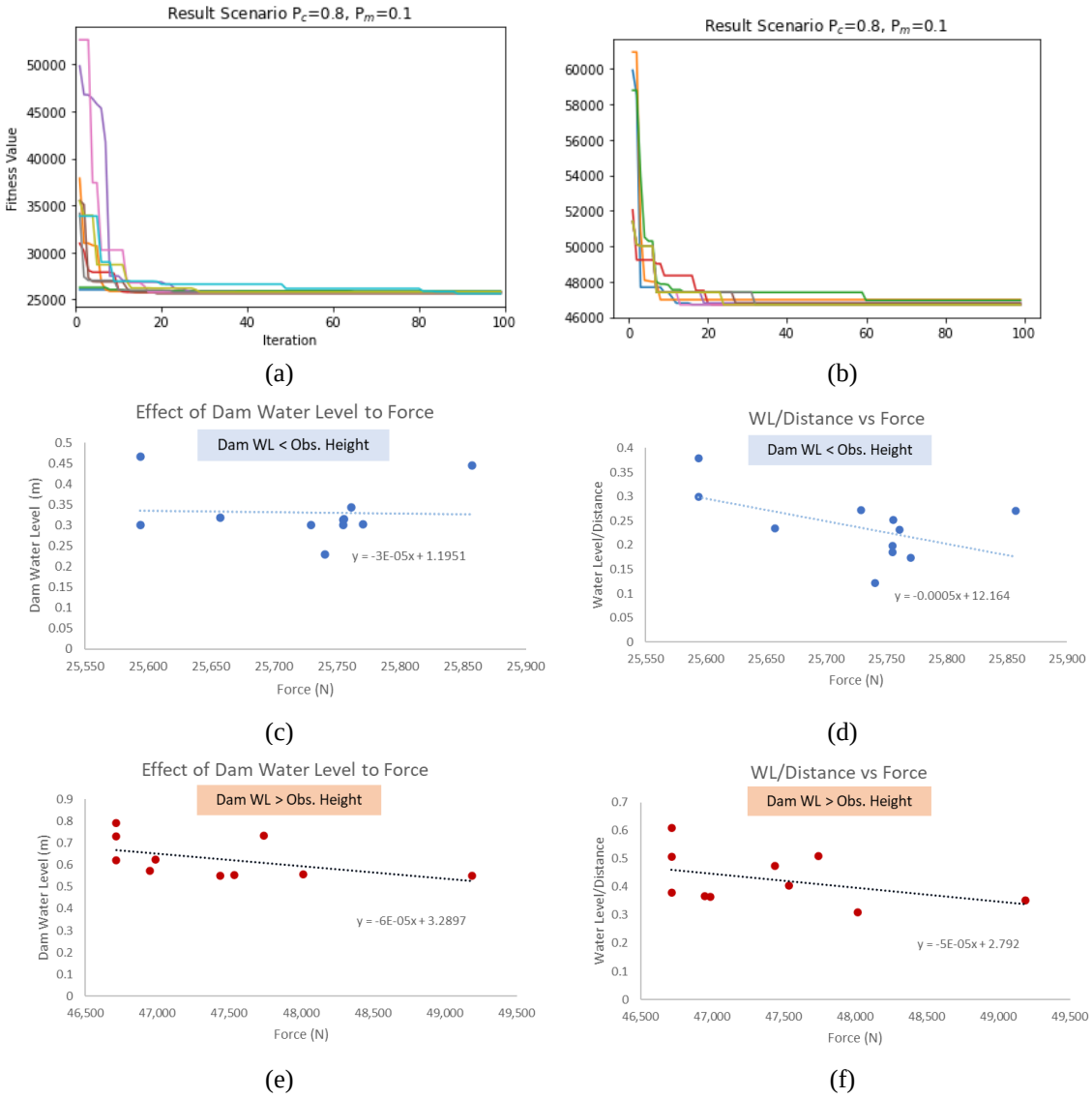

Fig 10 The result of optimizing the initial dam water level and obstacle location; (a) fitness variation when initial dam water level is lower than the structure height, (b) fitness variation when initial dam water level is higher than the structure height, (c) effect of dam water level to force (WL<Str. Height), (d) effect of distance to force (WL<Str. Height), (e) effect of dam water level to force (WL>Str. Height) and (f) effect of distance to force (WL>Str. Height)

Given the computational demands of optimization, there is a pressing need to reduce computational time. Hence, we've employed a 1D numerical model and a simplified numerical scheme. However, this approach may lead to inaccuracies due to its failure to account for lateral water flow. It's imperative to explore other forces acting around buildings, which may warrant expanding the model to 2D or 3D. Additionally, advanced numerical models can enhance accuracy in simulating dam break flows.

Further studies could delve into multi-building layouts to comprehensively understand lateral forces. Such research could offer valuable insights for urban planning and mitigation strategies, including evacuation routes. Additionally, future investigations should consider the impact of dam break failure mechanisms and reservoir shapes, as these factors significantly influence dam break flows, as highlighted in previous studies (Amini *et al.* 2017, Hu *et al*. 2020). These endeavors will contribute to a more comprehensive understanding of dam break phenomena and aid in the development of effective mitigation measures.

5. Conclusions

This study undertakes three optimization procedures to determine the optimal shape of an energy dissipator for minimizing force due to dam break flows. Among the shapes tested, the round shape with the arc facing downward emerges as the most effective dissipator, followed closely by the triangle shape. Conversely, the square shape proves to be the least efficient dissipator, potentially obstructing water flow and generating high impulse and impact forces.

While the optimum width remains consistent across all shapes at 0.9 m, the optimal structure height varies. The square shape necessitates the lowest height to minimize force, whereas the triangle and round shapes exhibit height ranges of 0.2-0.6 m and 0.2-0.9 m, respectively. This variation aligns with the potential energy dissipating capabilities of each shape, indicating that taller structures using the triangle and round shapes still achieve minimal force.

The force exerted on the energy dissipator increases with higher initial dam water levels, with a notable effect observed when the water level exceeds the dissipator's height. Conversely, when the initial dam water level is lower than the structure, force reduction of up to 53% is observed. Additionally, greater distance between the energy dissipator and the dam results in higher force exerted on the structure. Distance has a more significant influence in changing the proportion of velocity-induced force or pressure force acting on the structure.

Acknowledgments

The research described in this paper was financially supported by the research project (RS-2024-00356663) of Basic Science Research Program through the National Research Foundation of Korea (NRF) funded by the Ministry of Education.

References

Amini, A., Arya, A., Eghbalzadeh, A. and Javan, M. (2017), "Peak flood estimation under overtopping and piping conditions at Vahdat Dam, Kurdistan Iran", *Arab J. Geosci.*, **10**(6), 127. https://doi.org/10.1007/s12517-017-2854-y.

Biscarini, C., Di Francesco, S. and Manciola, P. (2010), "CFD modelling approach for dam break flow studies", *Hydrol. Earth Syst. Sci*., **14**(4), 705-718. https://doi.org/10.5194/hess-14-705-2010.

Bruce E., Ross B., Corotis, John B. and Nicholas P.J. (1993), "Assessing cost of dam failure", *J. Water Resour. Plann. Management*, **119**(1). https://doi.org/10.1061/(ASCE)0733-9496(1993)119:1(64).

Callum Phin (2018), Dam-break impact on support of coastal structures. University of Dundee, School of Engineering, Physics and Mathematics, Department of Civil Engineering.

Chanson, H. (2006), "Tsunami surges on dry coastal plains: Application of dam break wave equations", *Coast. Eng. J.*, **48**(4), 355-370. https://doi.org/10.1142/S0578563406001477.

Chrysanti, A., Song, Y. and Son, S. (2023), "Comparative study of laminar and turbulent models for three-dimensional simulation of dam-break flow interacting with multiarray block obstacles", *J. Korea Water Resour. Assoc*., **56**(1), 1059-1069. https://doi.org/10.3741/JKWRA.2023.56.S-1.1059.

Delestre, O., Lucas, C., Ksinant, P.A., Darboux, F., Laguerre, C., Vo, T.N.T., James, F. and Cordier, S. (2013), "SWASHES: A compilation of shallow water analytic solutions for hydraulic and environmental studies", *Int. J. Numer. Meth. Fl.*, **72**(3), 269-300. https://doi.org/10.1002/fld.3741.

Hien, L.T.T. and Van Chien, N. (2021), "Investigate impact force of dam-break flow against structures by both 2D and 3D numerical simulations", *Water*, **13**, 344. https://doi.org/10.3390/w13030344.

Holland, J.H. (1975), Adaptation in natural and artificial systems, University of Michigan Press, Ann Arbor.

Hu, H., Zhang, J., Li, T. and Yang, J.A. (2020), "Simplified mathematical model for the dam-breach hydrograph for three reservoir geometries following a sudden full dam break", *Nat. Hazards*, **102**(3), 1515-1540. https://doi.org/10.1007/s11069-020-03979-w.

Hwang, S. and Son, S. (2023), "An efficient HLL-based scheme for capturing contact-discontinuity in scalar transport by shallow water flow", *Commun. Nonlinear Sci. Numer. Simul.*, **127**, 107531. https://doi.org/10.1016/j.cnsns.2023.107531.

Issakhov, A., Zhandaulet, Y. and Nogaeva, A. (2019), "Numerical investigation of the dam break flow for optimal form of the obstacle by VOF method", *Proceedings of the AIP Conference*, AIP Publishing.

Jung, T. and Son, S. (2023), "A study on terminological definition of tsunami in Korean", *J. Korea Water Resour. Assoc*., **56**(5), 363-371. https://doi.org/10.3741/JKWRA.2023.56.5.363.

Kocaman, S., Güzel, H., Evangelista, S., Ozmen-Cagatay, H. and Viccione, G. (2020), "Experimental and numerical analysis of a dam-break flow through different contraction geometries of the channel", *Water*, **12**(4), 1124. https://doi.org/10.3390/w12041124.

Liu, L., Sun, J., Lin, B. and Lu, L. (2018), "Building performance in dam-break flow – an experimental study", *Urban Water J.*, **15**(3), 251-258. https://doi.org/10.1080/1573062X.2018.1433862.

Noh, J. and Son, S. (2023), "Development of the sediment transport model using GPU arithmetic", *J. Korea Water Resour. Assoc*., **56**(7), 431-438.

Putri, P.I.D., Iskandar, R.F., Adityawan, M.B., Kardhana, H. and Indrawati, D. (2020), "2D shallow water model for dam break and column interactions", *J. Civil Eng. Forum*, **6**(3), 237-246. https://doi.org/10.22146/jcef.54307.

Saghi, H. and Lakzian, E. (2019), "Effects of using obstacles on the dam-break flow based on entropy generation analysis", *Eur. Phys. J. Plus*., **134**(5), 237. https://doi.org/10.1140/epjp/i2019-12592-3.

Soares-Frazão, S. and Zech, Y. (2008), "Dam-break flow through an idealised city", *J. Hydraulic Res*., **46**(5), 648-658. https://doi.org/10.3826/jhr.2008.3164.

Son, S. and Jung, T. (2022), "Statistical analysis of tsunamis from multiple faults sequential failure with different time intervals and geographical layouts", *Ocean Eng*., **250**, 110720. https://doi.org/10.1016/j.oceaneng.2022.110720.

Qian, X., Hwang, S. and Son, S. (2024), "A study on key determinants in enhancing storm surges along the coast: Interplay between tropical cyclone motion and coastal geometry", *J. Geophys. Res. Oceans*, **129**(2), p.e2023JC020400, https://doi.org/10.1029/2023JC020400.

MK